Three-dimensional transient numerical simulation of the solid volume fraction of a fluidized bed: the role of three solution orders using a discretization scheme

EDVCATIO PHYSICORVM
SIC ITVR AD ASTRA
QVO NON ASCENDAM ?

ISSN 1870-9095

L.P. Olivo-Arias[1], L.G. Araujo[2]
[1]*Instituto Politécnico Nacional, Centro de Investigación en Ciencia Aplicada y Tecnología Avanzada.*
Legaria No. 694 Colonia Irrigación, C.P. 11500 México D.F., México
[2]*Instituto de Pesquisas Energéticas e Nucleares, IPEN-CNEN/SP*
Av. Prof. Lineu Prestes, 2242-Butantã, São Paulo, SP CEP 05508-000, Brazil.

E-mail: lolivoa1500@alumno.ipn.mx

(Received 22 January 2021, accepted 17 May 2021)

Resumen

El solucionador de dinámica de fluidos computacional (DFC) FLUENT ha experimentado un amplio desarrollo para extender su robustez y precisión para una amplia gama de regímenes de flujo. Para eso, el solucionador FLUENT tiene un método numérico en el solucionador basado en presión que tradicionalmente se ha utilizado para flujos incompresibles y ligeramente compresibles. El algoritmo es basado en la presión que resuelve las ecuaciones de forma segregada o desacoplada. Este algoritmo ha demostrado ser robusto y versátil, y se ha utilizado en concierto con una amplia gama de modelos físicos, incluidos flujos multifásicos y transferencia de calor conjugada. Sin embargo, hay aplicaciones en las que la tasa de convergencia del algoritmo segregado no es satisfactorio, generalmente debido a la necesidad en estos escenarios de acoplamiento entre las ecuaciones de continuidad y momento. El objetivo de este artículo es validar el modelo Euleriano para determinar las fracciones volumétricas de la fracción de la fase sólida. Para eso, utilizamos datos de la literatura y el algoritmo (solver) PCSIMPLE a diferentes ordenes de solución de las ecuaciones de continuidad, momento y turbulencia. Además, determinamos su eficiencia en sistemas transitorios y cómo afectarían los resultados en la hidrodinámica de un reactor de lecho fluidizado trifásico. Los resultados fueron significativos, representando asi el fenómeno de interacción entre las fases líquido-sólido y sólido-gas.

Palabras claves: Dinámica de Fluidos Computacional, Reactor de Lecho Fluidizado de tres fases, Modelo Hidrodinámico.

Abstract

The FLUENT solver employed in the Computational Fluid Dynamics (CFD) has been extensively developed to extend its robustness and precision for a wide range of flow regimes. For that, the FLUENT solver has a numerical method in the pressure-based solver that has traditionally been used for incompressible and slightly compressible flows. The algorithm is based on the pressure that solves the equations in a segregated or decoupled mode. This algorithm has proven to be robust and versatile and has been used cooperatively with a wide range of physical models, including multiphase flows and conjugated heat transfer. However, there are applications in which the convergence rate of the segregated algorithm is not satisfactory, generally due to the need in these coupling scenarios between the continuity and momentum equations. The objective of this article is to validate the Eulerian model to determine the volumetric fractions of the solid phase fraction. For this, we used data from the literature and the PCSIMPLE algorithm (solver) at different orders of solution of the continuity, momentum, and turbulence equations. Also, we determined its efficiency in transient systems and how it would affect the results in the hydrodynamics of a three-phase fluidized bed reactor. The results were significant, thus representing the phenomenon of interaction between the liquid-solid and solid-gas phases.

Keywords: Computational Fluid Dynamics, Three-phase fluidized bed reactor, Hydrodynamic model.

I. INTRODUCTION

The volume fraction of phases is an important transport property of three-phase fluidized beds and one of the main parameters to evaluate the hydrodynamic behavior of this type of system. This behavior reflects the complex and individual interactions of the phases, such as fluid-fluid or fluid-solid momentum exchange during the bed expansion process.

For many processes, the solid volume fraction is a crucial hydrodynamic parameter when there are particle suspension and entry of gas and liquid flows. In these cases, there is the

interaction between flows, such as gas-solid, liquid-solid, solid-solid, and the attrition of the particles and the domain wall, generating sediments and material wear.

The estimation of hydrodynamic parameters plays an important role in the modeling, simulation, design, and control of three-phase fluidized bed reactors. However, the estimation is often limited by the lack of reliable measurement techniques. Such techniques are essential to obtain laboratory-scale data to validate with and develop correlations to study the hydrodynamic behavior of industrial reactors [1]. Therefore, researchers employ tools such as Computational Fluid Dynamics (CFD) to provide design information. This information is necessary to describe variables with time and space, which can apply to multiphase systems.

Important parameters on three-phase studies are the volume fraction of the solid phase, involving physical models, chemical kinetics, and phenomenological models for the evaluation of the hydrodynamic parameter. For this study, we considered a real gas to simulate a real fluidization phenomenon, which would occur in a laboratory-scale reactor. We also incorporated different conditions of three-dimension (3D) meshing and discretization schemes.

CFD is the most successful tool to determine these varieties of hydrodynamic parameters. To obtain an agreeable simulation, reliable physical models are necessary to calculate the converged solution. The process of discretization transforms partial differential equations into a system of algebraic equations. There are dozens or even hundreds of discretization methods of partial differential equations. The main techniques for discretization are the finite volume method, the finite element method, finite differences, among others. Next, the method of discretization of finite volume and its general aspects will be discussed.

The available literature provides several mathematical correlations that describe fluidized bed processes. These models depend on the application because there is not a unique model with universal applicability. A complex set of equations that shall be analyzed before commencing the solving procedures for a very precise description of the process. One important aspect to evaluate the fluidized bed system is the hydrodynamic study.

Some articles [2, 3] analyzed a fully functional 3D, CFD simulation, of the gas separation region in an ebullated bed reactor transient system. Their results provided a framework to compare future designs, as well as evaluating fundamental insights in the separation dynamics in the freeboard region of this reactor.

Gas volume fraction model predictions were compared against commercial data previously reported. The phase distribution shows a high gas volume fraction region at the apex of the vessel and under the skirt, as previously reported by [3]. In these simulations, it is assumed that the vessel is originally full of liquid and is brought to steady-state conditions following a step-change in the inlet gas fraction. The dynamic response of the ebullated bed reactor to a gas inlet velocity produced step changes, from 0.0 to 0.3 m s^{-1}, in the volumetric fraction. Initial conditions of the gas volumetric fractions of 5, 10, 20, 30, 40, and 50 % were used to assess the relative impact on the system hydrodynamics during the liquid–gas separation. As the gas volume fractions increased, the primary factor affecting the separation efficiency was the displacement of liquid volume, which reduced the overall liquid phase momentum.

As a result, more gas entrainment occurred at lower inlet gas phase fractions. This effect was primarily due to the constant overall phase velocity used, where the liquid volume flow rate is increased to maintain the constant total flow as the gas fraction is reduced. This behavior is responsible for generating higher velocities in the recycle cup and more gas entrainment at equivalent recycle ratios.

A 3D transient model was already reported, simulating the local hydrodynamics of a three-phase fluidized bed reactor (liquid-gas-solid) using the CFD method [4]. The CFD simulation predictions were compared to the experimental data reported by other authors [5]. The flow field predicted by CFD simulations showed fair agreement with the experimental results. The gas volume fraction profile predicted by the researchers matches closely with the experimental data reported by[6], at the center region of the column and slightly varies at the wall region of the column. This may be due to the effect of the wall on the gas volume fraction. The researchers concluded that the gas volume fraction profile decreases when the radial position increases.

The simulation of the fluidized system and the effect of different superficial gas velocities, interactions of fluid-fluid and fluid-solid phases employs the k-epsilon standard turbulence model. Research available in the literature [7, 8, 9], was consulted as a reference to the fundamental theory to develop the numerical simulations hereby reported.

Most of the literature on CFD focused on a two-dimensional (2D) study, a two-phase system, and atmospheric conditions. Nonetheless, the contribution of this research is on a three-phase fluidized bed system, with real gas conditions using data from literature [1]. For that, our system is validated by low and high gas volume fractions as the initial conditions. Consequently, the present research is based on the study of real conditions and contributes to future simulations in real designs of fluidized bed systems using this type of computational model. In future simulations, it will be possible to examine liquids or different materials such as atmospheric and vacuum residues, and bitumen.

II. FLUIDIZED BED REACTOR SCHEME

The problem consists of a three-phase fluidized bed in which air and liquid (water) enter at the bottom of the domain.

The bed consists of solid material (glass beads) of uniform diameter, which forms a desired height in the bed. We simulated a gas-liquid-solid fluidized bed of diameter 0.1 m and height 1.88 m using commercial CFD software package FLUENT 18.2. The simulation has been done for static bed heights of 21.3 cm with glass beads of diameter 2.18 mm (Figure 1).

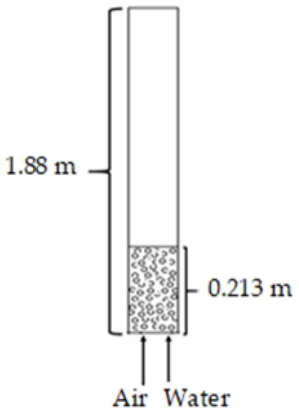

FIGURE 1. Fluidized bed reactor dimensions.

The process starts when the gas (air or hydrogen) and liquid (water) are injected at the bottom at different superficial gas velocities keeping fixed the value of the superficial liquid velocity. The starting time is set after contact between the solid phase and the inlet flows, followed by the mix between the phases and the suspension of particles along the column. The variables investigated in this work are the gas and solid volume fractions, which are validated by data from the literature [1]. The physical properties of materials employed in this investigation are shown in Table I.

TABLE I. Properties of air, water and glass beads used in simulations. *Reference (Fluent 18.2 data).*

Phase	*Density* $(kg \cdot m^{-3})$	*Viscosity* $(kg \cdot (m \cdot s)^{-1})$
Air	1.225	1.789×10^{-5}
Water	998.2	1.003×10^{-3}
Glass beads	2470	Same as water
Hydrogen	0.08409	8.4×10^{-4}

III. HYDRODYNAMIC MODEL

The simulation of the fluidized bed was performed by solving the governing equations of mass and momentum using the Fluent 18.2 CFD software, under the following assumptions:

- The application of the multifluid Eulerian model coupled to the kinetic theory for solid-phase, which considers the conservation of mass and momentum for the liquid, gas, and fluid phases [1].
- The solid phase is considered as non-porous spherical particles and the bubble distribution is negligible.

The governing equations available in the literature are briefly displayed below [4, 10, 11, 12].

A. Mass conservation

The mass conservation, for the fluidized bed system is given by the next equation:

$$\frac{\partial}{\partial t}(\alpha_j \rho_j) + \nabla \cdot (\alpha_j \rho_j \vec{u}_j) = 0, \quad (1)$$

where, ρ_j, α_j, and u_j are the mass density, volume fraction, and velocity of phase j = l, g, s, (liquid, gas, and solid, respectively). The volume fraction of the three phases should consider that:

$$\alpha_l + \alpha_g + \alpha_s = 1. \quad (2)$$

B. Momentum conservation

Momentum equations include terms such as pressure gradient (P), gravity acceleration ($\vec{g}$), tensor stress ($\bar{\bar{\tau}}_r$), and interphase force terms (K_{rp}). For the gas, liquid and solid phases, respectively, are represented by Equations (3-5), as follows:

$$\frac{\partial}{\partial t}(\alpha_l \rho_l \vec{u}_l) + \nabla \cdot (\alpha_l \rho_l \vec{u}_l \vec{u}_l) = -\alpha_l \nabla P + \nabla \cdot \bar{\bar{\tau}}_l + \alpha_l \rho_l \vec{g} + \sum_{p \neq l} K_{lp} \cdot (\vec{u}_l - \vec{u}_p), \quad (3)$$

$$\frac{\partial}{\partial t}(\alpha_g \rho_g \vec{u}_g) + \nabla \cdot (\alpha_g \rho_g \vec{u}_g \vec{u}_g) = -\alpha_g \nabla P + \nabla \cdot \bar{\bar{\tau}}_g + \alpha_g \rho_g \vec{g} + \sum_{p \neq g} K_{gp} \cdot (\vec{u}_g - \vec{u}_p), \quad (4)$$

$$\frac{\partial}{\partial t}(\alpha_s \rho_s \vec{u}_s) + \nabla \cdot (\alpha_s \rho_s \vec{u}_s \vec{u}_s) = -\alpha_s \nabla P + \nabla \cdot \bar{\bar{\tau}}_s + \alpha_s \rho_s \vec{g} + \sum_{p \neq s} K_{sp} \cdot (\vec{u}_s - \vec{u}_p). \quad (5)$$

C. K-epsilon Turbulence Model

The transport equations were solved numerically in the turbulent flow regime. Therefore, it is necessary to model the turbulent energy exchange and dissipation. To do this, the k-epsilon model and the wall function standard were taken into consideration [1,2,4].

$$\frac{\partial}{\partial t}(\rho_l k) + \frac{\partial}{\partial x_j}(\rho_l k u_l) = \frac{\partial}{\partial x_j}\left[(\mu + \frac{\mu_t}{\sigma_k})\frac{\partial k}{\partial x_j}\right] + G_k - \rho\varepsilon + S_k, \quad (6)$$

$$\frac{\partial}{\partial t}(\rho_l \varepsilon) + \frac{\partial}{\partial x_j}(\rho_l \varepsilon u_l) = \frac{\partial}{\partial x_j}\left[(\mu + \frac{\mu_t}{\sigma_\varepsilon})\frac{\partial \varepsilon}{\partial x_j}\right] + C_{1\varepsilon}\frac{\varepsilon}{k}G_k - C_{2\varepsilon}\rho\frac{\varepsilon^2}{k} + S_\varepsilon, \quad (7)$$

where G_k, represents the generation of turbulence of kinetic energy given to the velocity gradients; $C_{j\varepsilon}$ are constants, and σ_k and σ_ε are the turbulence numbers of Prandtl; and S_k and S_ε, are source terms.

D. Turbulence Viscosity Model

The viscosity of turbulence or Eddy is calculated by combining *k* and ε, as follows:

$$\mu_{t} = \rho C_{\mu} \frac{k^2}{\varepsilon}, \quad (8)$$

$$P_k = -\rho \overline{u_i' u_j'} \frac{\partial u_j}{\partial x_i}, \quad (9)$$

$$P_k = \mu_t S^2. \quad (10)$$

Where P_k the production of (*k*), and *S* is the modulus of the mean rate-of-strain tensor, defined as:

$$S \equiv \sqrt{2 S_{ij} S_{ij}}. \quad (11)$$

Also, the effect of buoyancy is given by:

$$P_b = \beta g_i \frac{\mu_t}{P_{rt}} \frac{\partial T}{\partial x_i}. \quad (12)$$

In the previous expressions, P_{rt} is the turbulent Prandtl number for energy —for the standard and realizable models, the default value of P_{rt} is 0.85—, g_i is the component of the gravitational vector in the *i*-th direction, and the coefficient of thermal expansion, β, is defined as:

$$\beta = -\frac{1}{\rho}\left(\frac{\partial \rho}{\partial T}\right)_p. \quad (13)$$

In the previous equations, the standard values $C_{1\varepsilon}$ = 1.44, $C_{2\varepsilon}$ = 1.92, $C\mu$ =0.09, σ_k =1.0 and σ_ε =1.3 were employed, during numerical simulation.

E. Spatial discretization

The first step in the application of computational fluid dynamics consists of the spatial discretization of the domain to, later on, calculate the numerical approximation of the convective and diffusive flows, as well as the sources. There are many methods for the discretization of the problem. The methods of discretization require a previous geometric discretization (spatial) so that it is possible to perform the discretization of the equations that govern the fluid. There are two types of meshing: structural and unstructured mesh.

F. Discretization (Interpolation Methods)

Field variables (stored at cell centers) must be interpolated to the faces of the control volumes. Eq 14.

$$\frac{\partial(\rho\phi)}{\partial t} V + \sum_{f}^{Nfaces} \rho_f V_f \phi_f \cdot A_f = \sum_{f}^{Nfaces} \Gamma_\phi \nabla_{\phi_f} \cdot A_f + S_\phi V. \quad (14)$$

There are five main interpolation schemes for the convection term:

i. First-Order Upwind – Easiest to converge, only first-order accurate.
ii. Power Law – More accurate than first-order for flows when Recell < 5 (typ. low Re flows) .
iii. Second-Order Upwind – Uses larger stencils for second order accuracy, essential with tri/tet mesh or when flow is not aligned with grid; convergence may be slower.
iv. Monotone Upstream-Centered Schemes for Conservation Laws (MUSCL) – Locally 3rd order convection discretization scheme for unstructured meshes; more accurate in predicting secondary flows, vortices, forces, etc.
v. Quadratic Upwind Interpolation (QUICK) – Applies to quad/hex and hybrid meshes, useful for rotating/swirling flows, 3rd-order accurate on uniform mesh.

In this study, the first, the second and the fourth order were employed in the PC Simple solver. For the governing equations, further explanation will be given.

G. SIMPLE Algorithm

First Order vs. Second Order.
Flow may be aligned with the grid or not. For the former (e.g., laminar flow in a rectangular duct modeled with a quadrilateral or hexahedral grid), the first-order upwind discretization may be acceptable. For the latter, such as when it crosses the grid lines obliquely, first-order convective discretization increases the numerical discretization error (numerical diffusion). For triangular and tetrahedral grids, since the flow is never aligned with the grid, the second-order discretization is usually the method of choice. For quad/hex grids, the second-order discretization is also the best option, especially for complex flows.

In summary, while the first-order discretization generally yields better convergence than the second-order scheme, it generally will yield less accurate results, especially on triangular/tetrahedral grids.

For most cases, the second-order scheme can be applied since the start of the calculation. In some cases, however, the first-order scheme has to be used at the beginning and then switched to the second-order scheme after a few iterations. For example, if one is running a high-Mach-number flow calculation that has an initial solution much different than the expected final solution, a few iterations with the first-order scheme is needed and then one may swift to the second-order scheme and continue the calculation until convergence. For a simple flow that is aligned with the grid, the numerical diffusion will be low, so the first-order scheme is generally used instead of the second-order scheme without any significant loss of accuracy.

Finally, if convergence difficulties are observed or foreseen in the application of the second-order scheme, the first-order scheme should be employed instead.

H. QUICK Scheme

The QUICK scheme can be employed for computing a higher-order value of the convected variable ϕf at a face. This is the case for quadrilateral and hexahedral meshes, where unique upstream and downstream faces and cells can be identified. QUICK-type schemes are based on a weighted average of second-order-upwind and central interpolations of the variable [13].

IV. NUMERICAL METHODS

The 3D computational domain was discretized by hexahedral 100,000 cells for the fine mesh. The cell boundary layers are close to the walls where the velocity gradient increased, and a finer resolution was necessary. The maximum cells of these dimensions were found to be adequate to achieve mesh-independent results in a similar study performed by the Gidaspow, which employed the *k-epsilon* Standard turbulence model. The solution was initialized from all zones.

A solid volume fraction data were taken from experiments (i.e. the volume fraction of the solids in the part of the column up to which the glass beads were fed) and used for patching (see Figure 2).

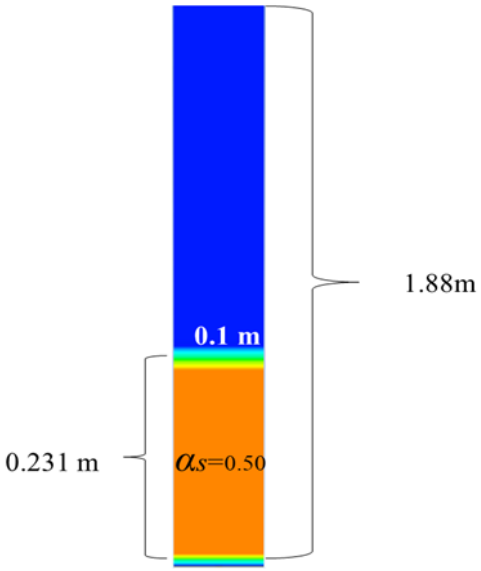

FIGURE 2. Domain-based Initialization.

In order to obtain the stability and convergence for multiphase simulations, the time step selected was 0.001 s with a maximum of 20 iterations per time step convergence. The details of the meshes used in this study are displayed in Table II.

TABLE II. Mesh quality and specifications for Minimum Orthogonal Quality.

Mesh O-grid	*Characteristics*
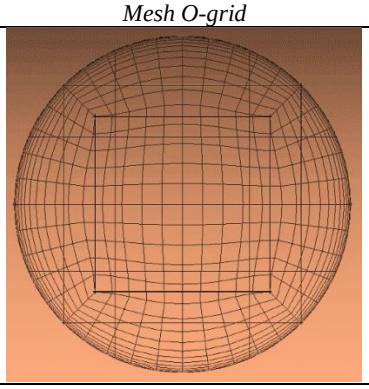	No. of Nodes: 104,721 100000 hexahedral cells Intermediate mesh size Mesh Quality MOQ = 7.26468 × 10^{-1}

For this research, the finite volume method was used to solve the system of governing equations. In order to solve the pressure-velocity coupling, the Phase-Coupled SIMPLE (PCSIMPLE) algorithm was employed. It is an extension of the SIMPLE algorithm to multiphase flows. Moreover, a second-order upwind and QUICK discretization schemes were used to determine the convection terms.

The computational geometry used for the simulation considers, as a general domain, a cylindrical region that contemplates a bottom gas inlet with a non-uniform parabolic velocity profile, and boundary conditions of outlet pressure (see Figure 3) with a fully developed gas flow. In the wall, a border condition of non-slip wall, both for the liquid phase and for the gas phase, was considered.

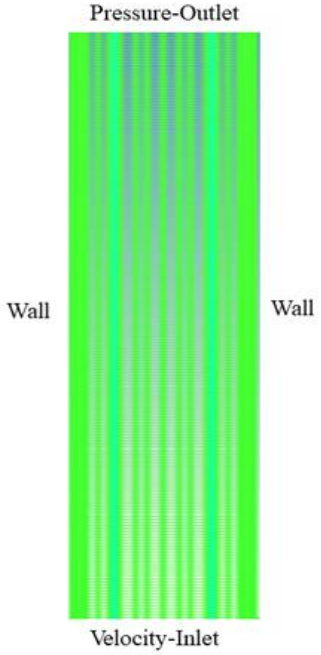

FIGURE 3. Boundary condition.

Table III shows the drag and turbulence models, and the boundary conditions.

TABLE III. The numerical simulation models.

Numerical methodology	Multiphase flow models
Drag formulation	Schiller-Naumann and Morsi-Alexander (fluid-fluid) Gidaspow (fluid-solid)
Turbulence model	k-epsilon standard model
Boundary conditions	Velocity-inlet No slip at the wall Pressure-outlet

V. RESULTS AND DISCUSSIONS

A mesh sensitivity study was performed to select suitable turbulence models and validate the air magnitude of velocity with different types of dimensions (2D and 3D). A high initial condition of gas volume fraction was established. In the first scenario, we simulated the process in severe conditions of pressure (1 MPa) to analyze the effect of the superficial gas and liquid velocities (v_g = 0.0125 and 0.05 m·s^{-1}), and (v_l = 0.12 m·s^{-1}) on this hydrodynamic parameter and associate it with a real behavior fluidized bed reactor. Table IV represents the physical and process simulation.

TABLE IV. Physical and process simulation.

Description	Value	Comment
Superficial gas velocities (m·s$^{-1)}$	0.015, 0.032, 0.05, 0.06 and 0.11.	Inlet boundary conditions
Superficial liquid velocity (m·s^{-1})	0.02, 0.06 and 0.12	Inlet boundary conditions
Static bed height (m)	0.231	Fixed value
Particle diameter (m)	0.00218	Fixed value

A. Effect at High Gas Volume Fraction Conditions

Validations were carried out between different discretization schemes (i.e. first, second upwind and QUICK) to observe the response of the hydrodynamic parameters and ensure the consistency of the solution. Then, the results of the volume fraction for the gas and solid phases were analyzed. Finally, a comparison between different drag models for the fluid-fluid interaction took into account a consideration of non-ideal gas at atmospheric and severe conditions.

The comparison was performed estimating a low and high initial condition for the volume fraction of the gas phase. The effect against the bed height during the fluidization process was also analyzed. According to [1], the first-order upwing discretization scheme was reported with Standard k-epsilon dispersed Eulerian multiphase model; standard wall functions were used and convergence and accuracy solution were reported. This can be seen in the plots of Figure 5. A convergence criterion of 10^{-3} was used here. The area-weighted average of solid volume fraction at 0.0125 m·s^{-1} of superficial gas velocity using the first-order discretization scheme validated the [1], and proposed models, employing a first-order upwind. It did not show a good trend, despite of its ability to converge (less accurate solver software). An initial condition of gas volume fraction in a three-phase system was established at 20%. It shows the effect of the superficial gas velocity over the gas volume fraction.

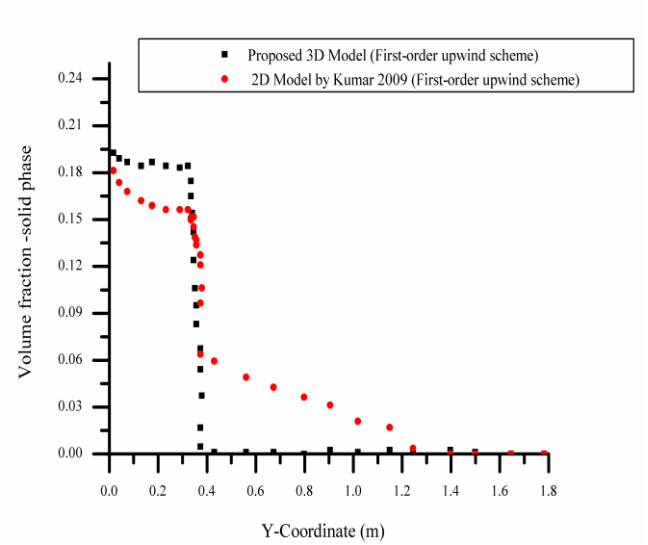

FIGURE 4. Area-weighted average X-Y plot of volume fraction of glass beads at 20% initial condition of gas volume fraction. Air velocity of 0.025 m·s^{-1} first order upwind discretization scheme.

An evaluation of different order discretization schemes was carried out (Figures 5-6), presenting the comparisons between the first and second order upwind and the Quick schemes in order to analyze the effects over the hydrodynamic parameters. The comparison showed that the second-order upwind/QUICK discretization schemes provided better results compared to the first-order upwind scheme. In this approach, a higher-order accuracy is achieved at 25 s at a superficial gas velocity of 0.05 m·s^{-1}.

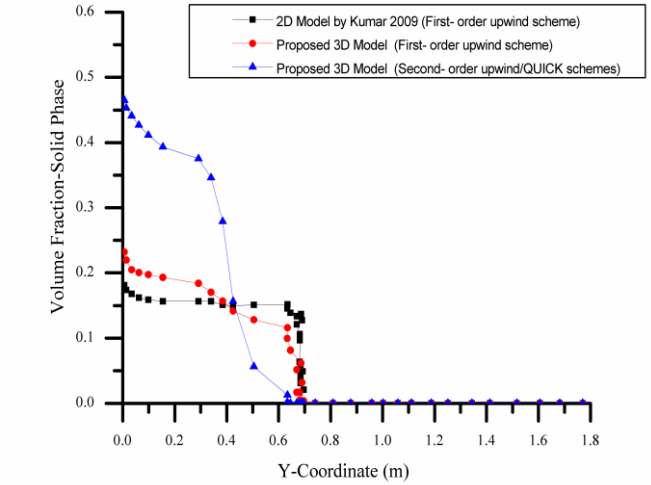

FIGURE 6. Area-weighted average X-Y plot of volume fraction of glass beads at 20% gas volume fraction initial condition, employing first and second order upwind/QUICK discretization schemes. Air velocity of 0.05 m·s^{-1}

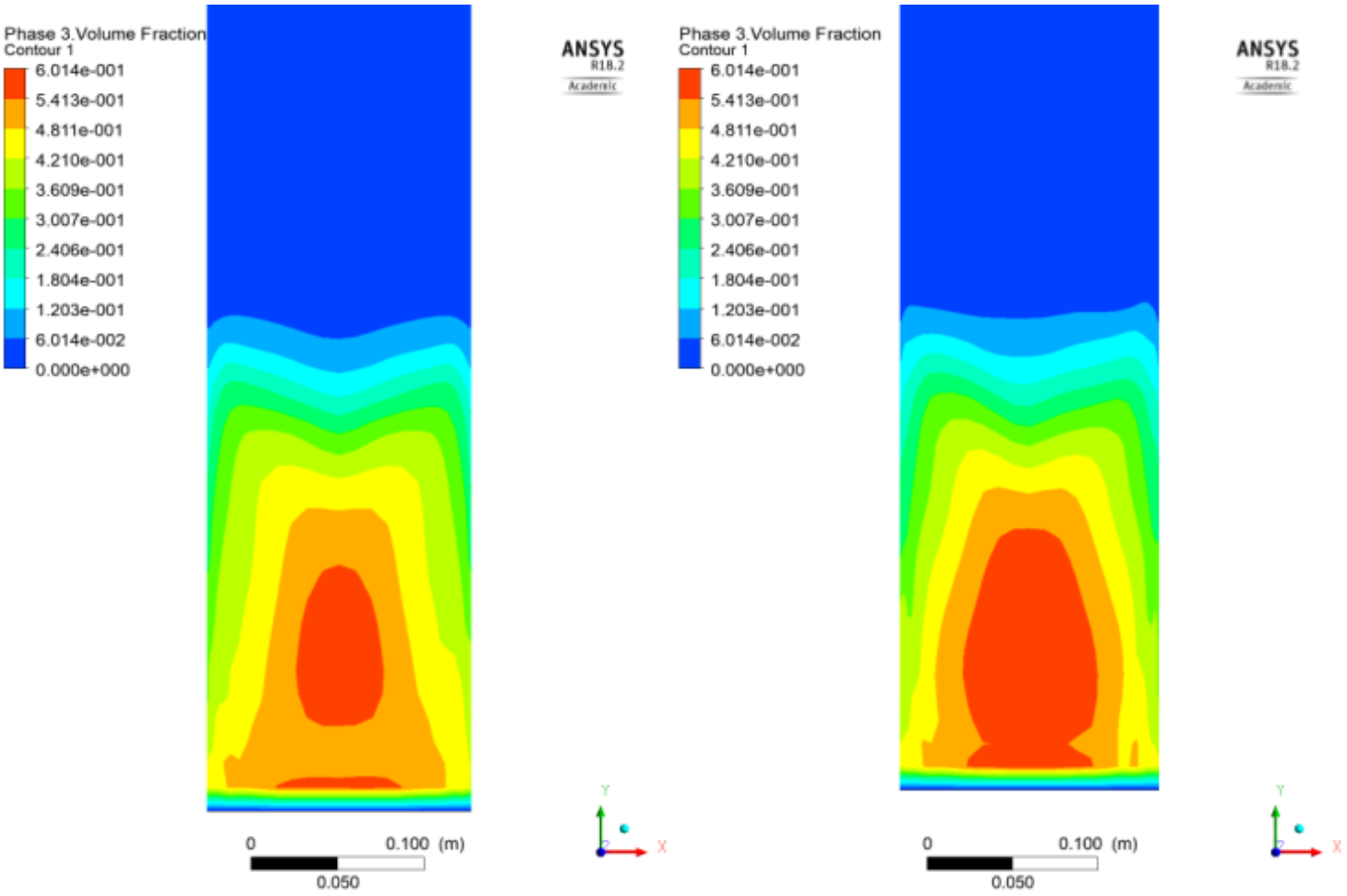

FIGURE 5. Contour of solid volume fraction first-order (left) and second order upwind/QUICK(right) schemes at superficial gas velocity 0.05 m·s^{-1} Gidaspow drag model until 25 s of simulation.

Numerical computations demonstrated the attractive properties of the approach for solutions with varying degrees of smoothness. The alternative approach was to develop all the simulations in order to reach better results for the validation for the experimental data. The result was overwhelming, using a higher order for the solution of spatial discretization schemes versus the results of 2D model [1], in first-order, which promotes numerical diffusion that can significantly change the final results. An increase in the initial gas volume fraction (20% to 50%) and the superficial gas velocity can be observed —keeping the values of both, the superficial liquid and gas velocities at 0.12 and 0.05 m·s^{-1}, respectively. Also, a contraction of the catalytic bed was observed by reducing the solid volume fraction. Otherwise, when low gas volume fraction was estimated, there was a slight bed expansion reaching a steady state. (Figure 7).

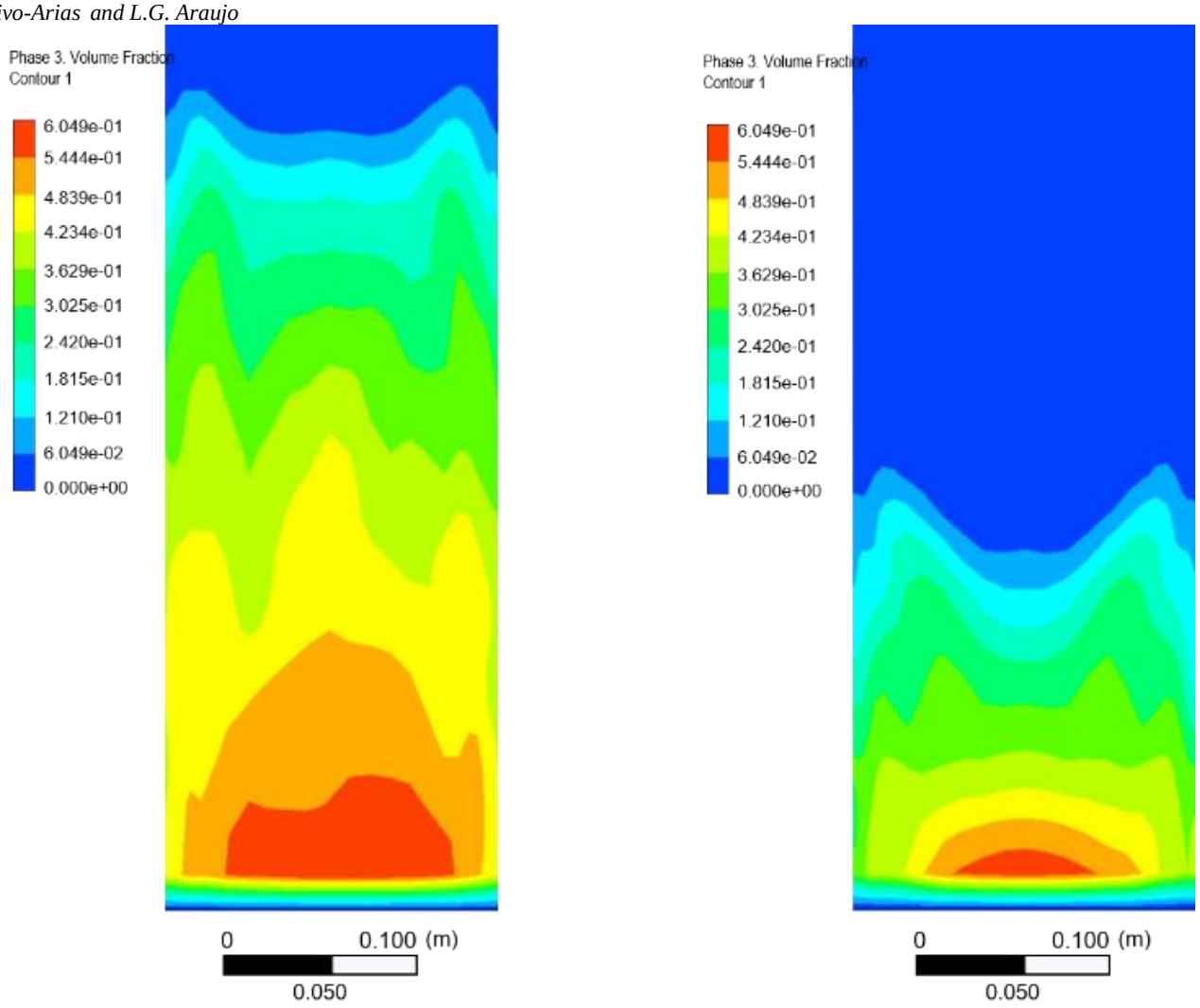

FIGURE 7. Contour of solid volume fraction at low (left) and high (right) gas volume fraction initial condition Gidaspow drag model 25 s of simulation.

Using the Shiller-Naumann drag model, it was observed that the gas volume fraction increased with a higher value of the superficial gas velocity. A rise in the superficial gas velocity was also observed to affect the internal flow structure, enhancing the mix in the bed and producing a more homogeneous bulk bed. In addition, whilst superficial gas velocity significantly affected fluidization hydrodynamics, changes in the superficial gas velocity did not significantly affect the fluidization symmetry (Figure 8).

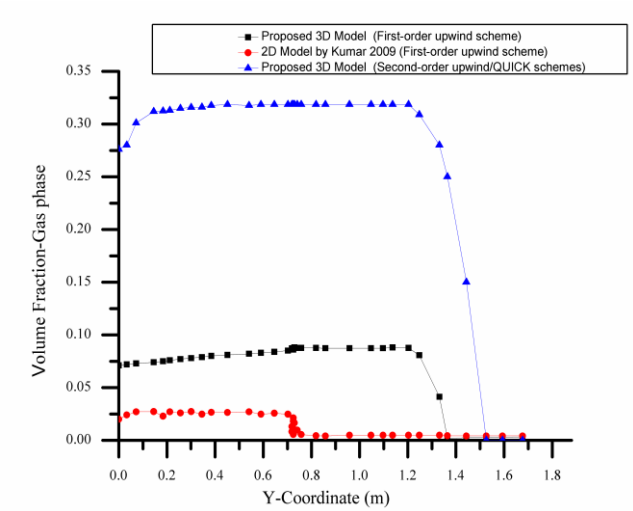

FIGURE 8. Area-weighted average X-Y plot of volume fraction of air with Shiller-Naumann model and 2D model [1] 2009, employing first and second order upwind/QUICK discretization schemes. Air velocity of 0.05 $m \cdot s^{-1.}$

Figure 9 presents the comparison between 2D and 3D model simulations for the validation of the air velocity variable. For inlet water velocity of 0.12 $m \cdot s^{-1}$ and an inlet air velocity of 0.0125 $m \cdot s^{-1}$, a parabolic pattern was observed. For the 2D model made by [1], the maximum air outlet was about 0.48 $m \cdot s^{-1}$ and for the proposed model, the maximum air velocity was 1 $m \cdot s^{-1}$. This demonstrated that the use of a higher order of discretization scheme and mesh allowed better results during the simulations even with lower air velocities. During the development of the equations, the wall velocity was zero. By working in different dimensions and by solving governing equations, the results were improved when the low superficial gas velocity was zero, due to the border non-slip wall conditions.

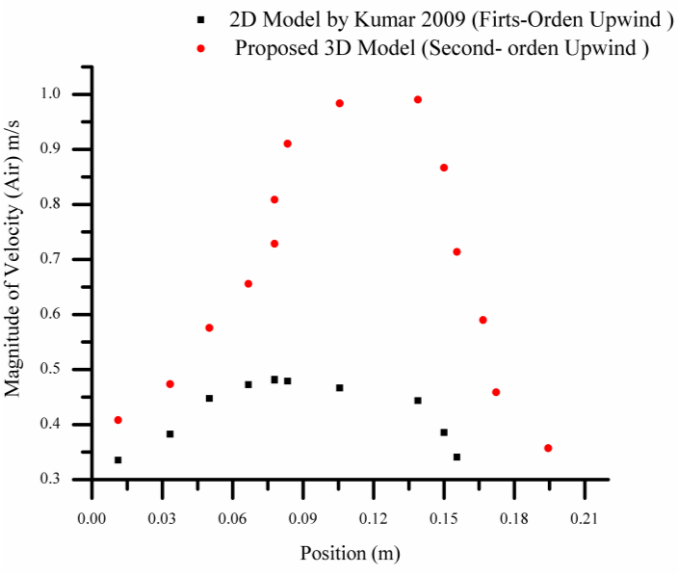

FIGURE 9. XY plot air magnitude of velocity in 2D and 3D, for a superficial gas velocity of 0.015 $m \cdot s^{-1}$.

VI. CONCLUSIONS

There are several CFD simulations that frequently take into account the ideal gas condition. Nonetheless, this consideration does not reflect the expected behavior in complex processes such as the fluidization process. In this case, there are high bed expansions, distant values of the volume fractions of the phases, low kinetic energy dissipations -among other phenomena. Validations based on literature were performed, in a three-phase fluidized bed reactor. We compared the dimensions (2D and 3D), spatial discretization schemes, and the initial and operating conditions that may affect the hydrodynamic parameters.

The behavior of the transient state of the fluidized beds of liquid-solid-gas was studied during this investigation. To validate the 2D model previously presented in the literature, the average cross-section profiles were compared with the values corresponding to the experimental data. This comparison showed that the model can predict reasonably well the hydrodynamic behavior of the fluidized bed for the volume fractions of the gas and solid phase. These models were used during the research of the three-phase fluidized bed hydrodynamics in computational fluid dynamics, and the standard k-epsilon was the model that reflected the best behavior.

The results represented for the fraction of solid and gas volume for first-order and second-order upwind schemes (continuity, turbulence and energy equations) and QUICK (momentum equation), suggest that the validation conducted in 3D model does not denote any inconsistency with the selected model. Better results were obtained by using higher order of discretization schemes. The superficial velocity and the initial estimates of parameters affected the gas volume fraction and a small contraction of the bed was observed when the initial condition of the gas volume fraction was increased.

The momentum interchange was analyzed by evolution and distribution along the catalytic bed, employing the Shiller-Naumann correlation. This is the most suitable model to evaluate the fluidization process.

Simulation results indicated a uniform distribution of the solid phase in the cross-section in 25 s of real flow time to allow a fluidization process. The contour of the solid volume fraction showed an ascend at the center of the bed and a descend near the walls. This represents an effect on operation variables at atmospheric conditions.

ACKNOWLEDGMENT

This work was supported by CONACYT and The Research Center for Applied Science and Advanced Technology (CICATA) both from Mexico.

REFERENCES

[1] Kumar, A., CFD modeling of gas–liquid–solid fluidized bed, (B. Tech, NIT, Rourkela, India, 2009).

[2] Lane, C. D., McKnight, C. A., Wiens, J., Reid, K., & Donaldson, A. A., *Parametric analysis of internal gas separation within an ebullated bed reactor*, Chemical Engineering Research and Design **105**, 44-54 (2016).

[3] McKnight, C. A., Hackman, L. P., Grace, J. R., Macchi, A., Kiel, D., & Tyler, J., *Fluid Dynamic Studies in Support of an Industrial Three-Phase Fluidized Bed Hydroprocessor*, The Canadian Journal of Chemical Engineering **8**, 338-350 (2003).

[4] Panneerselvam, R., Savithri, S., & Surender, G. D., *CFD simulation of hydrodynamics of gas–liquid–solid fluidised bed reactor*, Chemical Engineering Science **64**, 1119-1135 (2009).

[5] Kiared, K., Larachi, F., Chaouki, J., Guy, C., *Mean and Turbulent Particle Velocity in the Fully Developed Region of a Three-Phase Fluidized Bed*, Chemical Engineering & Technology **22**, 683-689 (1999).

[6] Yu, Y. H., Kim, S. D., *Bubble characteristics in the radial direction of three-phase fluidized beds*, AIChE Journal **34**, 2069-2072 (1988).
[7] Akita, K., Yoshida, F., *Gas Holdup and Volumetric Mass Transfer Coefficient in Bubble Columns. Effects of Liquid Properties*, Industrial & Engineering Chemistry Process Design and Development **12**, 76-80 (1973).
[8] Bhaga, D., Pruden, B. B., Weber, M. E., *Gas holdup in a bubble column containing organic liquid mixtures*, The Canadian Journal of Chemical Engineering **49**, 417-420 (1971).
[9] Kara, S., Kelkar, B. G., Shah, Y. T., Carr, N. L., *Hydrodynamics and axial mixing in a three-phase bubble column*, Industrial & Engineering Chemistry Process Design and Development **21**, 584-594 (1982).
[10] Kong, L., Zhang, C., & Zhu, J., *Evaluation of the effect of wall boundary conditions on numerical simulations of circulating fluidized beds*, Particuology **13**, 114-123 (2014).
[11] Du, W., Bao, X., Xu, J., & Wei, W., *Computational fluid dynamics (CFD) modeling of spouted bed: Assessment of drag coefficient correlations*, Chemical Engineering Science **61**, 1401-1420 (2006).
[12] Krishna, R., Ellenberger, J., *Gas holdup in bubble column reactors operating in the churn-turbulent flow regime*, AIChE Journal **42**, 2627-2634 (1996).
[13] ANSYS FLUENT 12.0 User's Guide. <https://www.afs.enea.it/project/neptunius/docs/fluent/html/ug/main_pre.htm> Acessed 28 July 2020.